Table S1. Oligonucleotide sequences. All oligonucleotides were purchased from Integrated DNA Technologies (IDT) and resuspended in nuclease free water prior to their use.

Supplementary Figure 1. RNAi expression cassettes. Depicted above are the four RNAi expression platforms that were tested for intracellular production of mature anti-*ATXN3* miRNA mimics. The miR-Atx3-148 platform is composed of the human miR-124a precursor sequence flanking the anti-*ATXN3* siRNA duplex. The sh-Atx3-148 platform is based on the recommendations provided by the Invitrogen Block-iT system. The –basal seq platform is similar to the miR-Atx3-148 platform except that is missing most of the basal stem sequence. Finally, the –loop seq platform contains the miR-124 basal stem sequence but lacks the entire miR-124 precursor loop sequence.

Supplementary Figure 2. miR-Atx3-148 suppression of a Luciferase/ATXN3-3'UTR fusion construct. (a) The human ATXN3 3'UTR was cloned into the pMIR-REPORT™ Luciferase vector as depicted. **(b)** U6-driven variants described in **Fig. S1** carrying a control (missense) or an anti-*ATXN3* miRNA mimic (148) were co-transfected together with the Luciferase/ATXN3-3'UTR fusion vector into HEK293 cells. Protein lysates were analyzed 48-hr post-transfection with an anti-Luc antibody (top blot, Luc). Tubulin levels were used to control for total protein loading (Tub). A representative blot is shown. Mean (% of control) and std. dev. of four independent experiments are listed below each lane.

Supplementary Figure 3. Off-target potential analysis for miR-Atx3-148. (**a**) A web algorithm, siRNA Sequence Probability-of-Off-Targeting Reduction (siSPOTR, https://sispotr.icts.uiowa.edu/sispotr/index.html), was used to identify transcripts (Gene ID) with a greater than 20% probability (TPOTS) of being silenced or "off-targeted" by miR-Atx3-148 expression. The analysis is based on the number and type of miR-Atx3-148 miRNA binding seeds (8mer, 7mer-M8, 7mer-1A or 6mer) present in the 3'UTR of these mouse transcripts. We used the Cerebellar Development Transcriptome Database (http://www.cdtdb.neuroinf.jp/CDT/Top.jsp) in order to establish the relative expression levels of these transcripts in the cerebellum of an adult mouse (Cb expression). We limited our analysis to transcripts with medium to high levels of expression in the adult mouse cerebellum (boxed). (**b**) Quantitative PCR analysis of the eight transcripts identified in (a) using RNA obtained from untreated (SCA3 TG), control treated (SCA3 TG-Ctrl) and miR-Atx3-148 treated (SCA3 TG-148) transgenic mice. Expression of miR-Atx3-148 did not significantly alter the expression levels of any of the analyzed transcripts. (**c**) Quantitative PCR analysis showed that expression of miR-Atx3-148 in SCA3/84.2 transgenic mice did not lead to an up-regulation of Iba-1 or Gfap mRNA levels, suggesting a lack of an overt inflammatory response. Error bars= ± Std. Dev.

Supplementary Figure 4. Immunohistochemical analysis of SCA3/84.2 mice. (**a**) In 2-month old littermate control mice, murine Ataxin-3 appears diffusely throughout the nuclei and soma of DCN neurons. In contrast, mutant human Ataxin-3 is predominantly found concentrated in the nuclei of DCN neurons in age-matched SCA3/84.2 transgenic mice. (**b**) Expression of rAAV-miR-Atx3-148 (hrGFP) in the DCN of SCA3/84.2 mice

does not alter the expression of E4B (red), a well-established Ataxin-3 interacting protein.

Supplementary Figure 5. Reduced nuclear mutant Ataxin-3 levels following miR-Atx3-148 expression in the cerebellum of SCA3/84.2 mice. (**a**) Shown are representative coronal cerebellar sections from control (AAV-miR-Ctrl, *n*=4) and RNAi-treated (AAV-miR-Atx3-148, *n*=4) SCA3/84.2 mice stained using the anti-Ataxin-3 1H9 antibody. Top panels are low magnification views of the deep cerebellar nuclei (DCN) ipsilateral or contralateral to the AAV injections. Squares (dashed and solid) represent areas used for the quantification of mutant Ataxin-3 staining in the DCN. The solid line square identifies the DCN region shown at higher magnification in the respective bottom panels. Nuclei of DCN neurons are strongly stained for mutant human Ataxin-3. (**b**) Compared to the contralateral non-injected DCN neurons, quantitative image analysis using NIH Image*J* revealed a greater than 80% reduction in the levels of nuclear Ataxin-3 staining in the neurons that reside in the injected DCN (ipsilateral to the AAV-miR-Atx3-148 injection). Error bars = ± Std. Dev.

Supplementary Materials and Methods

Cloning and expression of human ATXN3 3'UTR

The human *ATXN3* 3'-untranslated region was PCR amplified from human genomic DNA using primers listed on **TableS1**. After sequence verification, the amplicon was cloned into the SpeI-HindIII sites located downstream of a Luciferase reporter gene in the pMIR-REPORT™ Luciferase plasmid (Applied Biosystems). RNAi experiments

using this fusion vector and anti-Ataxin-3 RNAi molecules were performed as described on the main text.

Off-targeting potential analysis

To calculate the off-targeting potential of mir-Atx3-148 we utilize a web-based tool developed by the Davidson laboratory: https://sispotr.icts.uiowa.edu. The antisense sequence was used to perform a "POTS Lookup" analysis. The POTS score was 19.814 with a percentile of 95.2. The percentile represents the percent of total possible siRNA sequences that have a greater "off-targeting" potential. The analysis also provided a list of potential off-targets for mir-Atx3-148 and the number and type of potential miRNA-like binding seeds for mir-Atx3-148 present in the 3'UTR of these targets. We next analyzed the cerebellar expression level of potential off-targets exhibiting greater than a 20% chance of being silenced by mir-Atx3-148. This analysis was performed using cDNA microarray data from the *Cerebellar Development Transcriptome Database,* http://www.cdtdb.neuroinf.jp/CDT/Top.jsp. The expression of those transcripts showing medium to high levels of expression in the cerebellum of a 21-day old mouse (adult) was analyzed using RNA obtained from the cerebellum of SCA3/84.2 transgenic mice expressing mir-Atx3-148 using quantitative PCR as described in the main text.

Quantification of human mutant Ataxin-3 expression in the mouse DCN following expression of AAV-miR-Atx3-148.

Coronal sections from SCA3/84.2 transgenic mice unilaterally injected with AAV-miR-Ctrl or AAV-miR-Atx3-148 were stained with anti-Ataxin-3 1H9 antibody as described in the main text. In this case, incubation with an ALexaFluor-conjugated secondary antibody was replaced by the use of 3, 3'-diaminobenzidine as a substrate. SCA3/84.2 mice were 2-months of age at time of the injection and the cerebella were collected 8 weeks post-injection. To quantify the levels of nuclear mutant human Ataxin-3 staining in control treated and miR-Atx3-148 treated mice, the DCN was identified and photographed at low magnification. Images were processed using Image*J* software (RGB stacked>threshold settings>measurements) in order to quantify the % staining area (i.e. staining intensity) inside of a specified squared area (four square areas per DCN/section/mouse/4 mice per group= 16 measurements/group). Thresholds were set and quantification limited to the nuclear region of the DCN neurons. The % staining area numbers were calculated and reported as % of control (contralateral uninjected DCN).

miR-Atx3-148

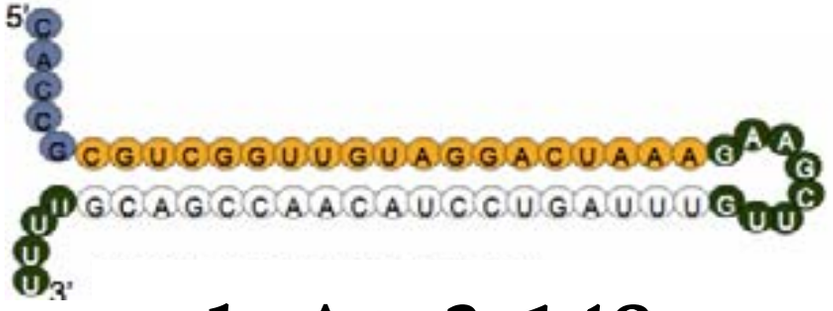

sh-Atx3-148

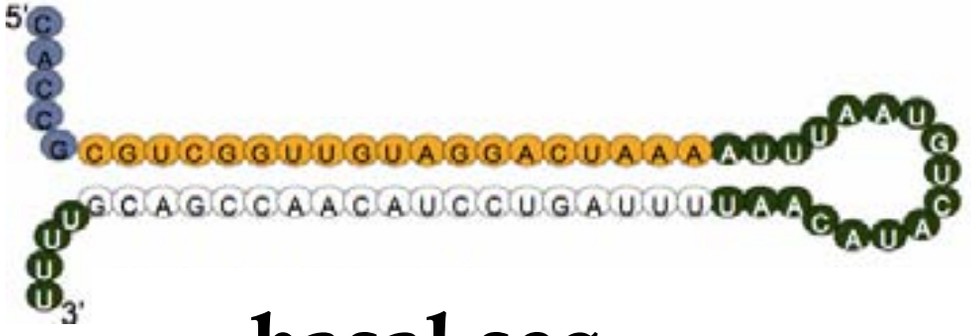

-basal seq

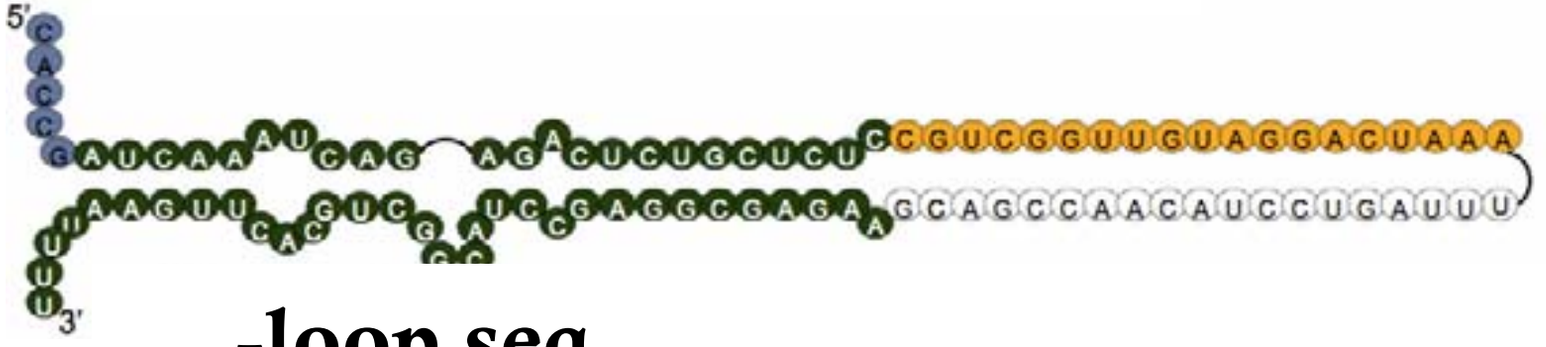

-loop seq

Plasmid Construct

Passenger strand

miR124 derived sequence

Guide strand

a


5’
LUC
3’
ATXN3-3’UTR

b

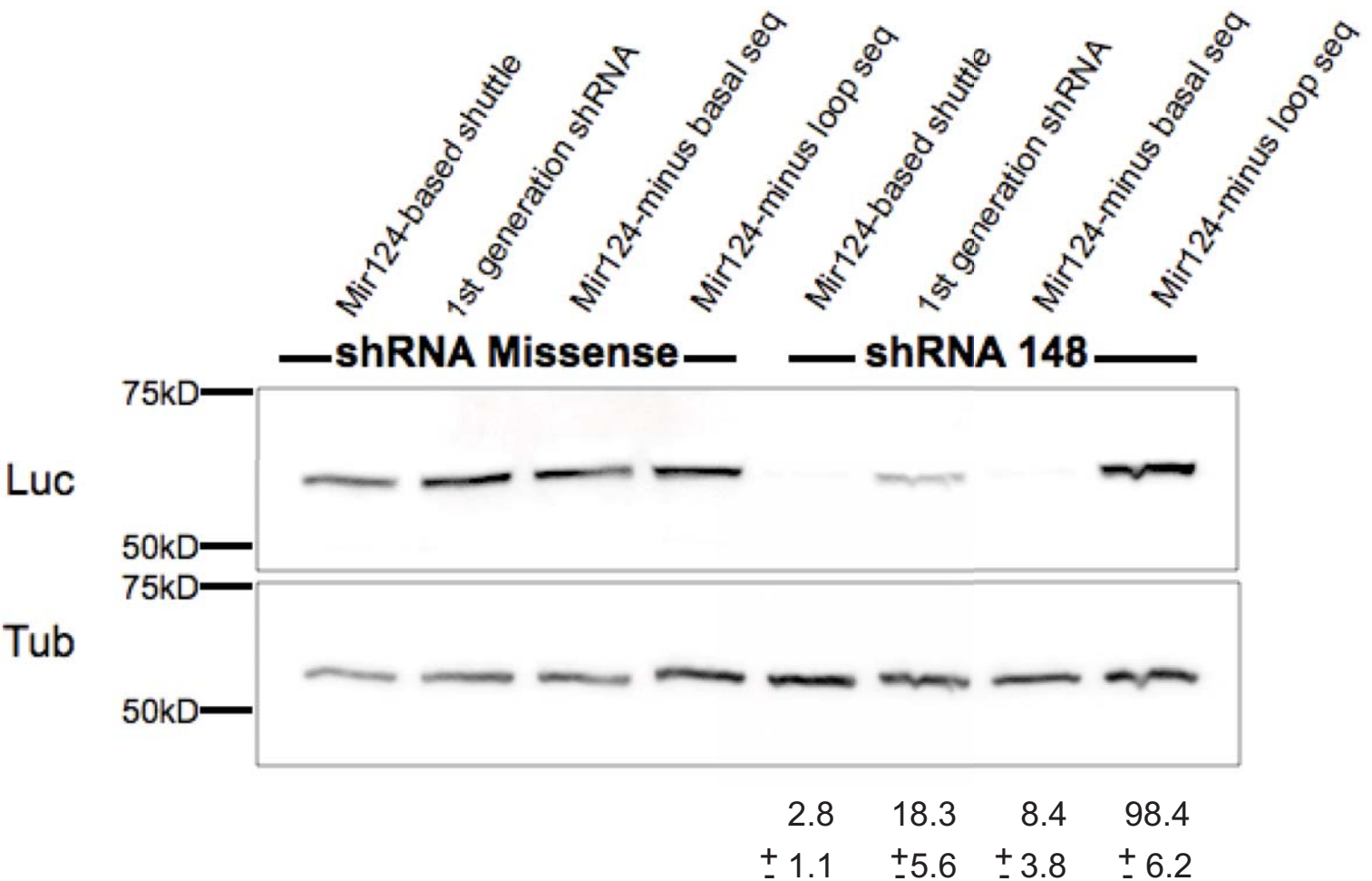
Mir124-based shuttle
1st generation shRNA
Mir124-minus basal seq
Mir124-minus loop seq
Mir124-based shuttle
1st generation shRNA
Mir124-minus basal seq
Mir124-minus loop seq
shRNA Missense
shRNA 148
75kD
Luc
50kD
75kD
Tub
50kD
2.8 ± 1.1
18.3 ± 5.6
8.4 ± 3.8
98.4 ± 6.2

a

Gene Symbol	TPOTS	miRNA seed binding type: 8mer	7mer-M8	7mer-1A	6mer	Cb Expression
Dcaf17	0.39	2	1	0		0 low
Iws1	0.39	2	1	0		0 low
Fbxl17	0.386	2	0	1		1 low
Tnrc6b	0.322	2	0	0		2 low
Onecut3	0.321	2	0	0		1 low
Ikbkap	0.321	2	0	0		1 med
Pcdhb5	0.32	2	0	0		0 low
Lonrf3	0.3	1	2	0		0 low
Pi15	0.297	1	1	1		2 low
Yy2	0.296	1	1	1		1 undetermined
Nav1	0.295	1	1	1		0 low
Samd8	0.295	1	1	1		0 med
Spire1	0.293	1	0	2		3 med
Zfp329	0.29	1	0	2		0 low
Secisbp2l	0.29	1	0	2		0 low
Ercc6	0.29	1	0	2		0 no
Chic1	0.27	0	2	2		0 low
Dlg2	0.27	0	2	2		0 high
Grk1	0.231	1	1	0		1 low
Uggt2	0.231	1	1	0		1 low
Krba1	0.231	1	1	0		1 low
C330019L16Rik	0.231	1	1	0		1 undetermined
D830031N03Rik	0.231	1	1	0		1 undetermined
Hoxc5	0.23	1	1	0		0 low
Ptges	0.23	1	1	0		0 low
Mis12	0.23	1	1	0		0 low
Med17	0.23	1	1	0		0 low
Cbx5	0.23	1	1	0		0 med
Itm2c	0.23	1	1	0		0 high
Sri	0.227	1	0	1		2 med
Tjp2	0.226	1	0	1		1 low
Eif2c1	0.226	1	0	1		1 low
Fzd3	0.226	1	0	1		1 low
Apol9a	0.225	1	0	1		0 low
Tectb	0.225	1	0	1		0 low
Trmt12	0.225	1	0	1		0 low
St6galnac3	0.225	1	0	1		0 low
Zfp142	0.225	1	0	1		0 low
Dcdc2a	0.225	1	0	1		0 low
Acp2	0.225	1	0	1		0 low
Kif21b	0.225	1	0	1		0 low
Stim2	0.225	1	0	1		0 low
Zdhhc21	0.201	0	1	2		1 low
Ikzf2	0.201	0	1	2		1 undetermined
Thsd7a	0.2	0	1	2		0 low
Galnt13	0.2	0	1	2		0 low
Socs7	0.2	0	1	2		0 high

b

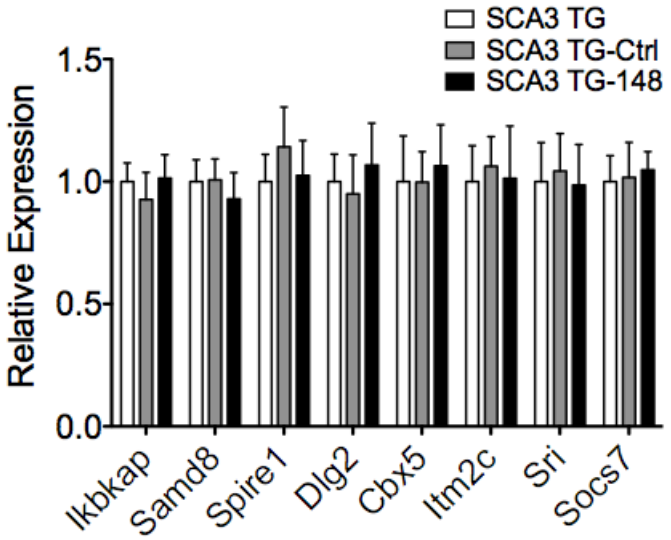

c

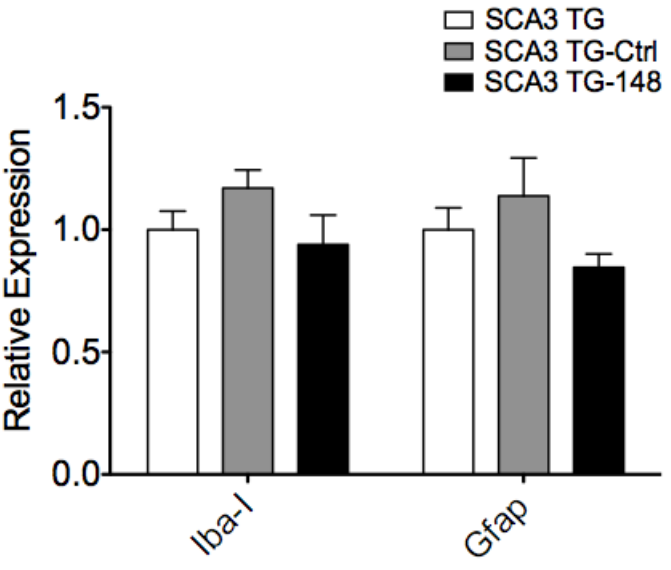

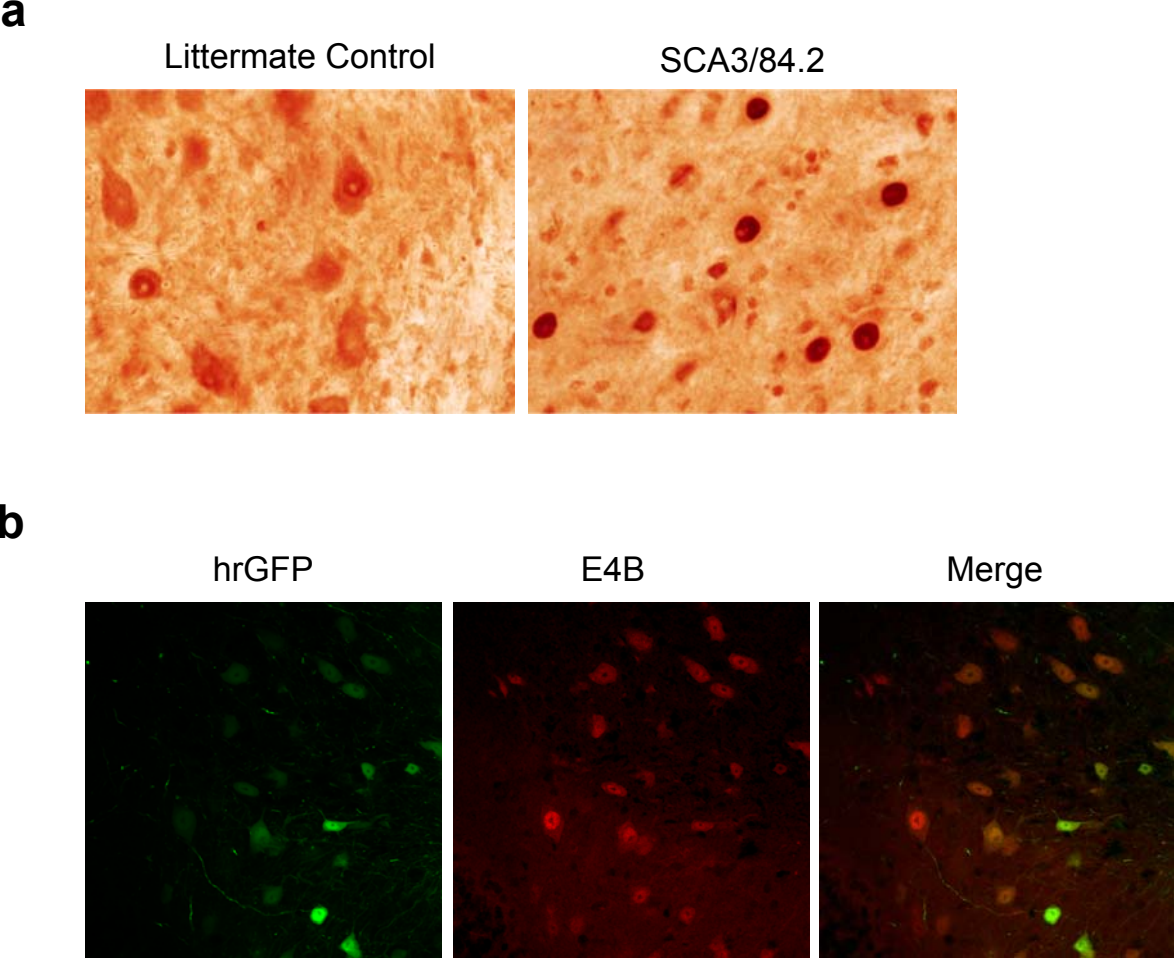
a
Littermate Control
SCA3/84.2
b
hrGFP
E4B
Merge

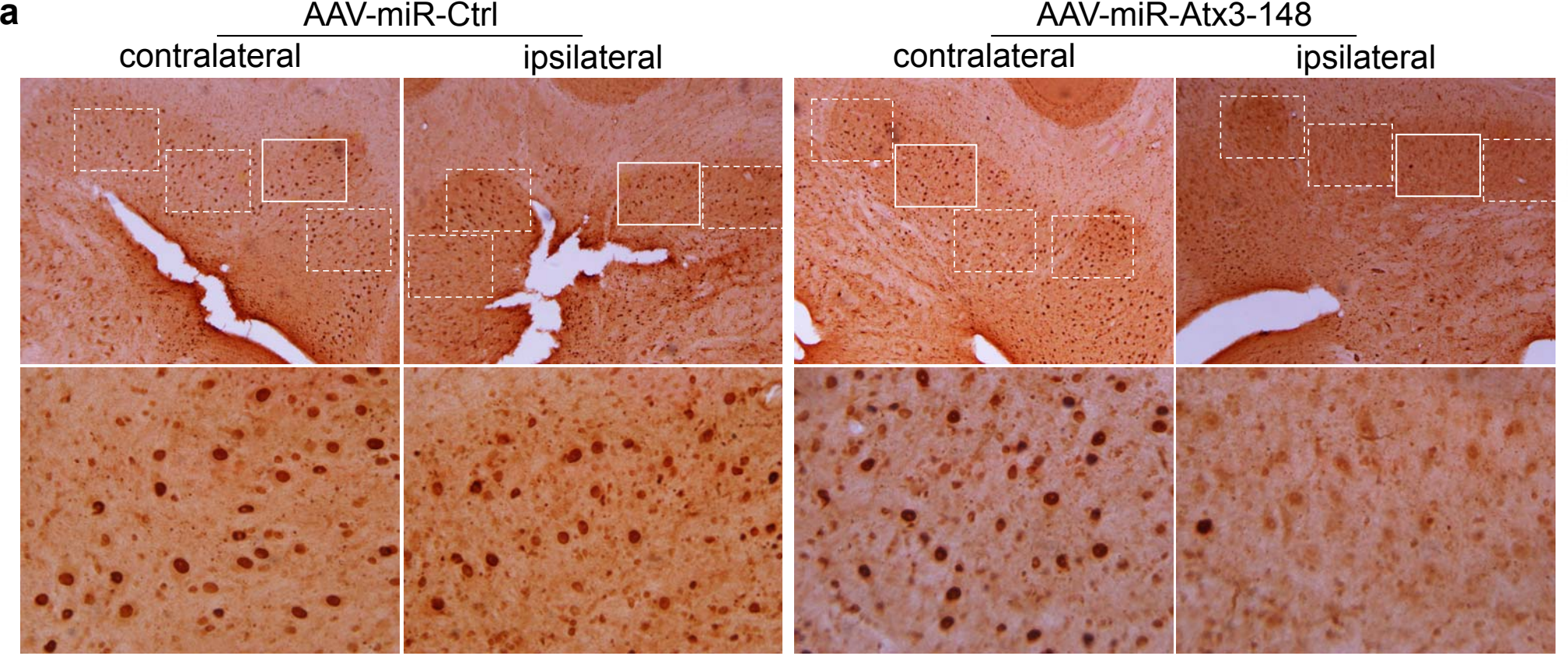
a
AAV-miR-Ctrl
AAV-miR-Atx3-148
contralateral
ipsilateral
contralateral
ipsilateral

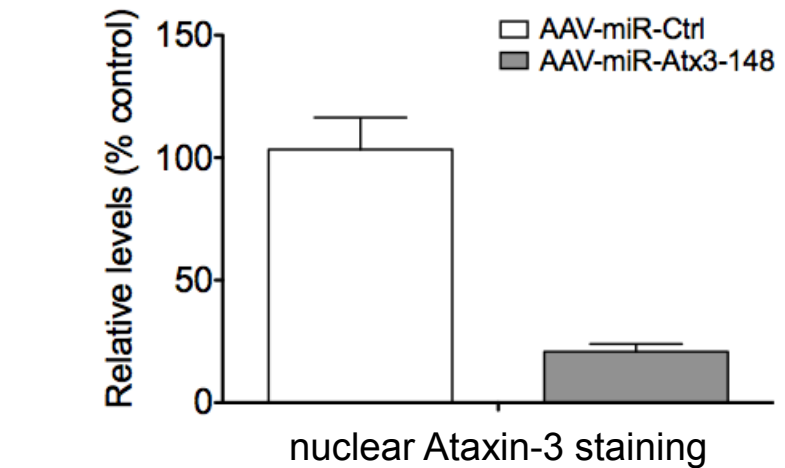
b
AAV-miR-Ctrl
AAV-miR-Atx3-148
Relative levels (% control)
150
100
50
0
nuclear Ataxin-3 staining